Journal of Optoelectronics and Advanced Materials Vol. 7, No. 6, December 2005, p. 3063 - 3067

MAGNETIC ANISOTROPY AND MAGNETOTRANSPORT PROPERTIES OF NANOSTRUCTURED Fe-Pt THIN FILMS

V. Georgescu*, C. Ilioaia, R. Muşat

Faculty of Physics, Al. I. Cuza University, Iasi, Romania

The study of magnetic and electrical characteristics of some nanostructured magnetic thin layers has fundamental importance to understand magnetization dynamics and is related to applications in magneto-electronics devices. This paper is devoted to the investigation of Fe-Pt alloy films with the aim to obtain by electrolysis nanostructured films with GMR effect. The Fe-Pt samples were prepared onto polycrystalline Cu substrates using electrodeposition with controlled potential, from a solution containing: K_2PtCl_6, $Fe(NH_4)_2(SO_4)_2$. $6H_2O$, H_3BO_3 and NaCl. The samples were characterised by torsion magnetometry, by an induction method, by SEM and EDAX. The studied samples showed uniaxial anisotropy perpendicular to the plane of the film. The nanostructured Fe_xPt_{1-x} films, with $x \approx 30 - 38$ % and granular morphology exhibit large values of the magnetoresistance (of about 11% in current perpendicular-to-plane configuration). Such electrodeposited alloys near to stoichiometric concentration $FePt_3$, are composed from antiferromagnetic clusters in addition to ferromagnetic ones, i. e. a mixed ferro- antiferro-magnetic state. The local concentration fluctuations generated during the film preparation results in a spatially inhomogeneous magnetic structure.

(Received August 25, 2005; accepted November 24, 2005)

Keywords: Nanotechnology; Electrodeposition; Nanostructured materials; Magnetic anisotropy.

1. Introduction

In the past few years, there are very interesting magnetic studies on nanostructured materials, focused on the interaction between the electron charges and magnetic spins [1, 2]. Giant magnetoresistance (GMR) in multilayers and metallic granular solids is therefore a very promising research direction. Our goal was to study nanocrystalline Fe-Pt films in a view to obtain by electrolysis nanostructured materials with GMR effect. The electrodeposition technique has major advantages over other methods of thin film production, namely, the possibility of performing deposition at normal conditions of pressure and temperature, requiring relatively inexpensive equipment. At the same time, it is possible that these nanostructured materials could be applied for magnetic sensors and magnetic recording.

The system of Fe-Pt alloys was chosen because there is a competition between ferro- and antiferro-magnetism in Fe-Pt [3], which could favour the GMR existence. It is known that the Fe-Pt phase diagram of bulk alloys displays at high temperatures a disordered fcc solid solution over the whole composition range, and at room temperatures two fcc ($L1_2$) ordered phases around the composition $FePt_3$ and Fe_3Pt, and one tetragonal ($L1_0$) ordered phase around the equiatomic composition FePt [4, 5]. This paper is concerned with films in the composition range of ordered ($L1_2$) $FePt_3$ phase. There are only few studies on magnetism of electrodeposited Fe-Pt films [6-9].

2. Experimental

All films were prepared by electrodeposition using the method previously described [6, 7]. The rate of electrodeposition was determined by interferometric microscopy and the film thickness was established as a function of the plating time. The composition and microstructure of

* Corresponding author: vgeor@uaic.ro

electrodeposited Fe-Pt films were characterized using EDAX and SEM techniques. The magnetic properties of the films were studied at room temperature using a torque magnetometer in fields up to 300 kA.m^{-1} and an a.c. induction Howling type device with computerised data acquisition system. The DC magnetoresistance measurements were performed applying the current perpendicular to the plane of the film (CPP configuration), by using a two-terminal platinum pressure contacts, and the external magnetic field was applied in the plane or perpendicular to the film plane. A digital multimeter HM 8112-2 type was used for resistance measurements. Field dependence of the magnetoresistance (MR) was defined as $MR(H) = 100[R(H) - R(H_{s+})]/R(H_{s+})$, where H_{S+} denotes the positive saturation magnetic field. The *MR (H)* curves in the figures of this paper start from the positive saturation field.

3. Results and discussion

The Fe-Pt films were electroplated on a copper substrate in shape of a disk (22 mm diameter) using an iron anode (with the same diameter). Iron and platinum ions were introduced in a single bath, containing: $Fe(NH_4)_2(SO_4)_2.6H_2O$, K_2PtCl_6, H_3BO_3 and NaCl, in double distilled water. The composition and thickness of the electrodeposited film from a solution containing Fe and Pt ions may be controlled by varying deposition parameters such as the cathode potential, the electrolysis duration and the concentration of the substances included in the electrolyte. The operating conditions of the bath were: pH=2.5, temperature T = (65±0.5) °C, without stirring the electrolyte.

We prepared a series of samples with the electrolysis parameters chosen as to obtain films in the composition range near to $FePt_3$ stoichiometric composition. We selected two typical samples (labelled A, and B) for magnetic characterisation and analysis in this paper, taking into account their mean composition (expressed as an average between the composition in the central part and the peripheral part of a sample). These samples contain: sample (A) ⟨29.750 %⟩ Fe, ⟨70.250 %⟩ Pt and sample (B) ⟨37.650 %⟩ Co, ⟨62.350 %⟩ Pt. Thus, the samples A and B have a composition in a domain range close to ordered phase ($L1_2$) $FePt_3$. The thickness of these films was of 250-300 nm, the same value for all the samples.

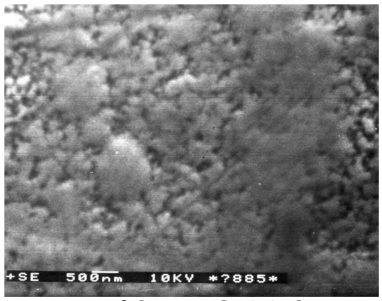

Fig. 1. Scanning electron microscopy of the sample (A) showing the multinuclear growth of the films. The marker bar shown in the image has a dimension of 500 nm.

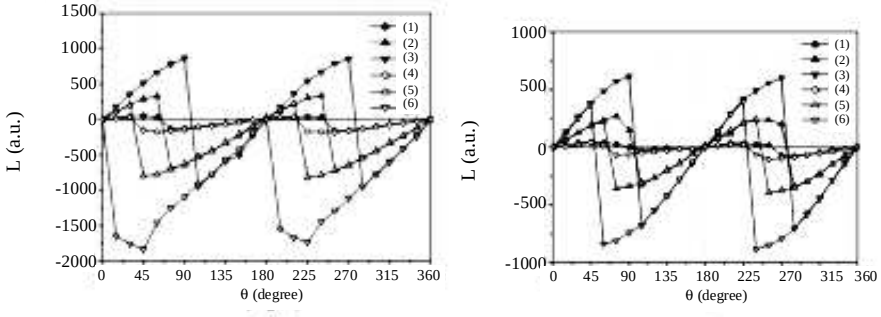

a b

Fig. 2. Torsion magnetometry curves for the samples A (fig. 2a) and B (fig. 2b) measured for the fields: 9.55 kA/m (curves 1, 4), 28.65 kA/m (curves 2, 5) and 95.5 kA/m (curves 3, 6). *H* rotates in a clockwise sense for curves (1, 2, and 3) and in the anticlockwise rotation for curves (4, 5 and 6).

A typical SEM image of the sample labelled (A) is shown in Fig. 1. The film is formed by multinuclear growth, containing grains with diameters less than 500 nm.

The magnetic anisotropy of the films was measured at room temperature with a torque magnetometer. Torque L on the samples is recorded as a function of the angle (θ) between the plane of the film and the applied magnetic field H. Figs. 2(a) and 2(b) show the static torque curves performed for clockwise and anticlockwise rotation of the magnetic field, for the samples A and B, respectively. The film plane was oriented perpendicular to the field-rotation plane, e. g. the torque was measured around an arbitrary axis parallel to the film plane, starting from the plane of the film ($\theta = 0$). The applied magnetic field was of 9.55 kA m^{-1} (for curves labelled 1 and 4), of 28.65 kA m^{-1} (curves 2 and 5), and 95.5 kA m^{-1} (curves 3 and 6). In Figs. 2(a) and 2(b), the curves labelled 1, 2 and 3 correspond to a clockwise rotation of the magnetic field and those labelled 4, 5 and 6 correspond to anticlockwise rotation.

The experimental torque curves exhibit mainly a twofold symmetry (the torque is proportional to sin 2θ), with a positive slope at $\theta = 0^o$ and a negative slope around $\theta = 90^o$. This indicates that the easy magnetization axis is perpendicular to the film plane. As the applied field increases, the torque curves become asymmetric, i. e. the rotational losses appear and they are measurable from the area enclosed by clockwise and anticlockwise curves. For fields exceeding the anisotropy field, the torque curves are asymmetric and irreversible. This behaviour could be ascribed to the antiferromagnetic type coupling between crystallites in the nanostructured samples. For alloys near to stoichiometric concentration $FePt_3$, there are also antiferromagnetic clusters in addition to ferromagnetic ones, growing from different nucleation centres.

The magnetic susceptibility measurements were performed using an a.c. induction Howling type device with computerised data acquisition system (50 Hz, maximum field of 57.3 kA/m applied in the plane of the samples). Two identical pick-up coils (one of them containing the sample) are used in series opposition to acquire the induced voltage. The differential susceptibility (χ) of the film is determined from the rate of change of field with time

$$\frac{dM}{dt} = \left(\frac{dM}{dH}\right)\left(\frac{dH}{dt}\right) = \chi\frac{dH}{dt} \tag{1}$$

The $dM/dt = f(t)$ curves were digitised (2048 sampling points) and analysed. Typical curves for the sample B are shown in Fig. 3a. The notation of the curves in the figure is the following: C1 – the output voltage of the Y1 channel, i.e. the magnetic susceptibility $\chi = (dM/dH) = f(t)$, C2 – the output voltage of Y2 channel, i.e. magnetic field $H = f(t)$ and C3 – integrated curve of the Y1 channel, i.e. the ascendant branch of the hysteresis loop, $M = f(t)$. The X-axis for curves C1, C2 and C3 is in time range 0-10 ms, and Y-axis is in arbitrary units. The hysteresis loop of the same sample (B) recorded in our device is shown in Fig. 3b, for a maximum field of 57.3 kAm^{-1}.

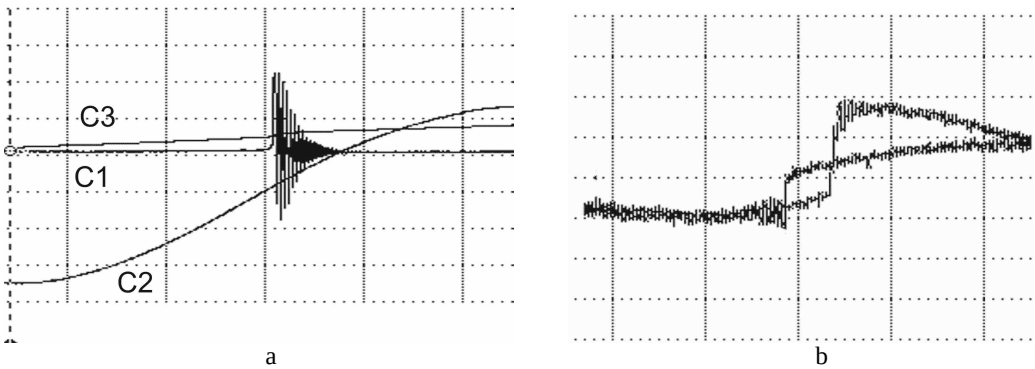

a b

Fig. 3a). Magnetic characteristic curves for the typical sample A. C1: dM/dt vs. t curve, C2: H vs. t, C3: integral curve. Scalation: C1=0.20V/div, C2=5.00V/div, C3=0.10V/div, OX=2ms/div. Fig. 3b). Hysteresis loop of the same sample. Scalation: OX=11.462kAm^{-1}/div and OY= arbitrary units.

The magnetotransport properties of the samples were measured at room temperature. The field dependence of the CPP magnetoresistance for the sample B, is presented in Fig. 4 for a

magnetic field applied in the film plane (a) and perpendicular to the plane (b). The CPP MR ratio is of about 10.72 % for our samples, with the similar kind of field dependence. The samples exhibit large magnetic Hall effect that can be deduced from different values of MR for different sense of magnetic field.

A number of studies of multilayers of iron and platinum using magnetisation measurements and Mössbauer spectroscopy have revealed information about the interactions of particles and surface effects. [9-12]. High uniaxial magnetocrystalline anisotropy is attributed to the large spinorbit coupling of the Pt atom and strong hybridisation of Pt d bands with highly polarised Fe d bands. The extraordinary Hall effect was observed also at room temperature in $Fe_{30}Pt_{70}$ thin films deposited on silicon (111) substrates by magnetron-sputtering technique [13]. We suppose that the large values of the magnetoresistance of the Fe_xPt_{1-x} (with $x \approx 30 - 38$ %) could be explained by a very strong spin-orbit interaction and a strong polarisation of the Pt *d* states induced by Fe atoms. The electric resistance of such samples in zero or low magnetic field (when the magnetic moments are preferentially antiferromagnetic coupled) is different from their resistance in a magnetic field, when the magnetic moments are ferromagnetic aligned, parallel to the field direction. The electrodeposited nanostructured alloys near to stoichiometric composition $FePt_3$ contain antiferromagnetic clusters in addition to ferromagnetic ones, i.e., they are in a mixed ferro- antiferro-magnetic state (mixomagnetic state). The local concentration fluctuations generated during the film preparation results in a spatially inhomogeneous magnetic structure.

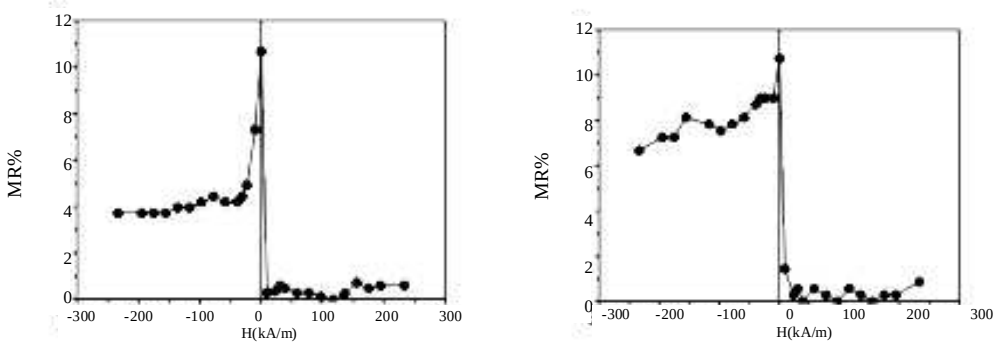

Fig. 4. Magnetoresistance as a function of magnetic field for the sample A (~$Fe_{30}Pt_{70}$) measured (a) in magnetic field parallel to the film plane; (b) in the field perpendicular to plane. The *MR (H)* curves start from the positive saturation field.

The magnetic inhomogeneity has a common feature; namely, it contains ferromagnetic phases separated by nonferromagnetic ones. Therefore, the enhancement of the magnetoresistance can be attributed to the spatially inhomogeneous magnetic structure having different magnetic component and to the exchange interaction between neighbouring interfaces. These effects depend on the polarization processes acting on the spin of conduction electrons, as well as on the magnetic configuration of the system.

4. Conclusions

We have prepared by electrolysis nanostructured Fe_xPt_{1-x} alloy films with $x = 30 - 38$ at% and a thickness of 250 - 300 nm, deposited onto Cu substrate. The films were magnetically characterized by recording the magnetic susceptibility curves in a.c. magnetic field (50Hz) parallel to film plane and by torque magnetometry. The magnetoresistance was determined for the current perpendicular to plan configuration (CPP), in magnetic field perpendicular, and parallel to the plane of the film. For the Fe_xPt_{1-x}, alloy films with $x \cong 30\%$ we have obtained high values for the magnetoresistance, indicating the possibility for future technological applications. The large values of magnetoresistance are due to the spatially inhomogeneous magnetic structure of the nanostructured materials and to the exchange interaction between neighboring grains.

References

[1] B. Szymanski, F. Stobiecki, Cryst. Res. Technol., **36**, 825 (2001).
[2] P. Allen, Solid State Communications, **102**, 127 (1997).
[3] G. Brown, B. Kraczek, A. Janotti, T. C. Schulthess, G. M. Stocks, D. D. Johnson, Phys. Rev. B **68**, 052405-8 (2003).
[4] A. Oles, F. Kajzar, M. Kucab, W. Sikora, Magnetic Structures determined by Neutron Diffraction, Panstwowe Wydawnictwo Naukowe, Warszawa (1976).
[5] A. Z. Menshikov, Yu. A. Dorofeyev, V. A. Kazantsev & S. K. Sidorov, Fiz. metal. Metalloved, **38**, 505 (1974).
[6] V. Georgescu, Analele Stiintifice ale Universitatii Al. I. Cuza din Iasi, Tom XXXII, s. I. B, Fizica, 9 (1986).
[7] V. Georgescu, M. Sorohan, Analele Stiintifice ale Universitatii Al. I. Cuza din Iasi, Tom XXXVIII, s. I. B, Fizica, 58 (1992).
[8] K. Leistner, J. Thomas, H. Schlorb, M. Weisheit, L. Schultz, S. Fahler, Appl. Phys. Letters, **85**, 3498 (2004).
[9] E. B. Svedberg, J. J. Mallet, S. Sayan, A. Shapiro, W. F. Egelhoff, Jr., T. Moffat, Applied Phys. Letters, **85**, 1353 (2004).
[10] A. Simopolous, E. Devlin, A. Kostikas, A. Jankowski, M. Croft, T. Tsakalakos, Phys. Rev. B **54**, 9931 (1996).
[11] A. Fnidiki, J. S. Douheret, J. Teillet, H. Lassri & R. Krishnan, J. Magn. Magn. Mat. **156**, 41 (1996).
[12] C. P. Luo, Z. S. Shan, D. J. Sellmyer, J. Appl. Phys. **79**, 4899 (1996).
[13] C. L. Canedy, G. Q. Gong, J. O. Wang, and Gang Xiao, J. Appl. Phys. **79**, 6126 (1996).